

Observation of the Quantum Zeno and Anti-Zeno Effects in an Unstable System

M. C. Fischer, B. Gutiérrez-Medina, and M. G. Raizen

Department of Physics, The University of Texas at Austin, Austin, Texas 78712-1081

(Received 30 March 2001; published 10 July 2001)

We report the first observation of the quantum Zeno and anti-Zeno effects in an unstable system. Cold sodium atoms are trapped in a far-detuned standing wave of light that is accelerated for a controlled duration. For a large acceleration the atoms can escape the trapping potential via tunneling. Initially the number of trapped atoms shows strong nonexponential decay features, evolving into the characteristic exponential decay behavior. We repeatedly measure the number of atoms remaining trapped during the initial period of nonexponential decay. Depending on the frequency of measurements we observe a decay that is suppressed or enhanced as compared to the unperturbed system.

DOI: 10.1103/PhysRevLett.87.040402

PACS numbers: 03.65.Ta, 03.65.Xp, 42.25.Kb, 42.50.Vk

Unstable quantum systems are predicted to exhibit a short time deviation from the exponential decay law [1–3]. This universal phenomenon led to the prediction that frequent measurements during this nonexponential period could inhibit the decay of the system, the so-called “quantum Zeno effect” [4–6]. More recently it was predicted that an enhancement of decay due to frequent measurements could be observed under somewhat more general conditions, which was named the “anti-Zeno effect” [7–10]. We report here the first observation of both the Zeno and anti-Zeno effects by repeated measurements during the nonexponential period of an unstable quantum system.

Our experiment consists of ultracold sodium atoms in an accelerated standing wave of light which creates an optical potential of the form $V_0 \cos[2k_L x - k_L a t^2]$, where V_0 is the amplitude of the potential, k_L is the wave number of the light forming the potential, x is the position in the laboratory frame, a is the acceleration, and t is time. Transformation to the frame accelerated with the potential (x') yields the form $V_0 \cos[2k_L x'] - \max'$ in which a constant inertial force on the atom with mass m is apparent. Classically, for a given amplitude V_0 and small enough acceleration, a atoms can be trapped inside this tilted “washboard potential” and be accelerated along with it. Quantum mechanically, an atom which is classically bound can escape from this trapped state into the continuum via tunneling [11–13]. The system is therefore unstable, and the decay would be expected to follow the universal exponential decay law. It was shown, however, that deviations from exponential behavior should occur for short times, owing to the initial reversibility of the decay process [1–3]. Our system is the only one in which these predicted deviations have been observed [14]. Improvements to our previous setup have now allowed us to explore parameter regimes for which much stronger deviations from the exponential behavior occur. This has enabled us to study the effect of repeated measurements on the decay of the system [4–6]. Even though measurement-induced suppression of the dynamics of a two-state driven system has been observed [15,16], no such effect was measured on an unstable sys-

tem. Frequent measurements during the decay of an unstable system are predicted to reduce or enhance the decay rate, depending on the measurement interval.

The experimental setup resembles the one used previously to study deviations from exponential decay and will be described only briefly. Several steps were necessary to prepare the initial condition. We started by cooling and trapping approximately 3×10^5 sodium atoms in a magneto-optical trap, followed by a stage of molasses cooling [17]. After this stage the distribution had a typical Gaussian width of $\sigma_x = 0.3$ mm in position and $\sigma_v = 6v_{\text{rec}}$ in velocity, where $v_{\text{rec}} = 3$ cm/s is the single-photon recoil velocity. After switching off the cooling and trapping fields the interaction beams were turned on. The interaction potential was a standing wave created by two linearly polarized counter-propagating laser beams with parallel polarization vectors. The light was far detuned from the $(3S_{1/2}) \leftrightarrow (3P_{3/2})$ transition in order to avoid electronic excitation and the resulting spontaneous emission. Detunings typically ranged from 40 to 60 GHz and the power in each of the beams was adjusted up to 150 mW. The beams were spatially filtered and focused to a beam waist of 1.8 mm at the position of the atomic cloud. Because of the large initial momentum spread of the atomic cloud, switching on the interaction potential populated several of the lower energy bands. Atoms projected into the lowest band are trapped within the potential wells, whereas atoms in the second band are only partially trapped. Atoms in even higher bands have energies well above the potential and hence are effectively free. To empty all but the lowest band, the standing wave was then accelerated to a velocity of $v_0 = 35v_{\text{rec}}$ by linearly chirping the frequency of one of the counter-propagating beams while keeping the frequency of the other beam fixed. As discussed in our previous work [11–13], accelerating the potential leads to a loss of population in the lower bands due to tunneling of atoms into higher untrapped bands. The transport acceleration a_{trans} was chosen to maximize tunneling out of the second band while minimizing losses from the first trapped band. This ensured that, after the initial acceleration, only the first

band still contained a significant number of atoms. After reaching the velocity v_0 the acceleration was suddenly increased to a value a_{tunnel} , where appreciable tunneling out of the first band occurred. This large acceleration was maintained for a period of time t_{tunnel} after which time the frequency chirping continued again at the decreased rate corresponding to a_{trans} . This separated in momentum space the atoms that were still trapped in the lowest band from those in the higher bands. After reaching a final velocity of $75v_{\text{rec}}$ the interaction beams were switched off suddenly. A diagram of the velocity profile versus time is shown in Fig. 1(a).

In the detection phase we determined the number of atoms that were initially trapped and what fraction remained in the first band after the tunneling sequence. After an atom tunneled out of the potential during the sequence, it would maintain the velocity that it had at the moment of tunneling. Turning off the light beams allowed the atoms to expand freely. During this period of ballistic expansion each atom moved a distance proportional to its velocity. Because of the difference in final velocity, trapped and tunneled atoms separated and could be spatially resolved. For imaging purposes the cooling beams were turned back on with no magnetic field gradient present. This temporarily restricted movement of the atoms in a “freezing molasses,” while the fluorescence was imaged onto a charge-coupled-device camera. Regions of the two-dimensional image were then integrated to obtain the desired fraction of remaining atoms over the number of initially trapped atoms. A typical integrated distribution is shown in Fig. 1(b). For this trace, about one-third of the initially trapped atoms have tunneled out of the well during the fast acceleration duration.

We observed the decay of the unstable system by repeating the experiment for various tunneling durations t_{tunnel} , holding the other parameters of the sequence fixed. The focus of this work, however, was the effect of measure-

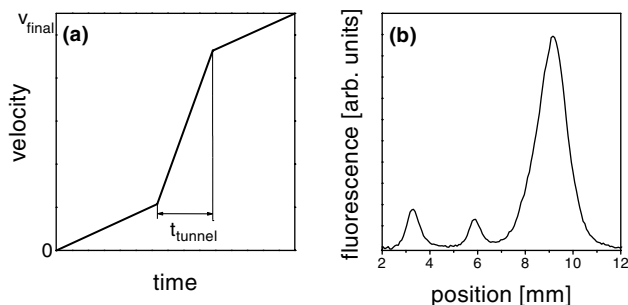


FIG. 1. Part (a) shows a diagram of the acceleration sequence. Part (b) shows a typical integrated spatial distribution of atoms after the time of ballistic expansion. The large peak on the right is the part of the atomic cloud that was not trapped during the initial acceleration. The center peak indicates the atoms that tunneled out of the optical potential during the fast acceleration period. The leftmost peak corresponds to atoms that remained trapped during the entire sequence. The survival probability is the area under the left peak normalized by the sum of the areas under the left and center peak.

ments on the system decay rate. The quantity to be measured was the number of atoms remaining trapped in the potential during the tunneling segment. This measurement could be realized by suddenly interrupting the tunneling duration by a period of reduced acceleration a_{interr} , as indicated in Fig. 2(a). During this interruption, tunneling was negligible and the atoms were therefore transported to a higher velocity without being lost out of the well. This separation in velocity space enabled us to distinguish the remaining atoms from the ones having tunneled out up to the point of interruption, as can be seen in Fig. 2(b). By switching the acceleration back to a_{tunnel} the system was then returned to its unstable state. The measurement of the number of atoms defined a new initial state, with the remaining number of atoms as the initial condition. The system must therefore start the evolution again with the same nonexponential decay features. The requirements for this interruption section were very similar to those during the transport section, namely the largest possible acceleration while maintaining negligible losses for atoms in the first band. Hence a_{interr} was chosen to be the same as a_{trans} .

Figure 3 shows the dramatic effect of frequent measurements on the decay behavior. The hollow squares indicate the decay curve without interruption. As pointed out by Misra and Sudarshan [4], one can take advantage of the slow initial decay in order to inhibit the decay altogether by frequently measuring the system at very short time intervals. They named this suppression of decay the quantum Zeno effect. The solid circles in Fig. 3 depict the measurement of the survival probability in which, after each tunneling segment of $1 \mu\text{s}$, an interruption of $50 \mu\text{s}$ duration was inserted. Only the short tunneling segments contribute to the total tunneling time. The survival probability clearly shows a much slower decay than the corresponding system measured without interruption. Care was taken to include the limited time response of the experimental setup into the analysis of the data. The response time

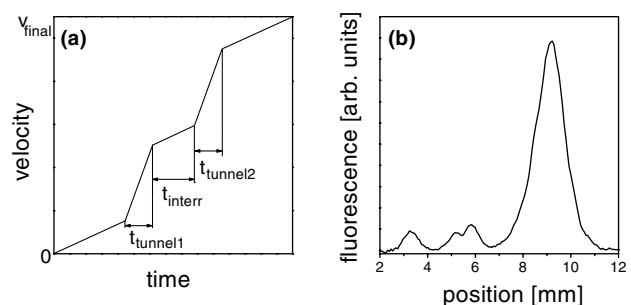


FIG. 2. Part (a) shows a diagram of the interrupted acceleration sequence. The total tunneling time is the sum of all the tunneling segments. Part (b) shows a typical integrated spatial distribution of atoms after the time of ballistic expansion. The peaks can be identified as in Fig. 1. However, the area containing the tunneled fraction of the atoms is now composed of two peaks. Atoms that left the well during the first tunneling segment are offset in velocity from the ones having left during the second period of tunneling. The amount of separation is equal to the velocity increase of the well during the interruption segment.

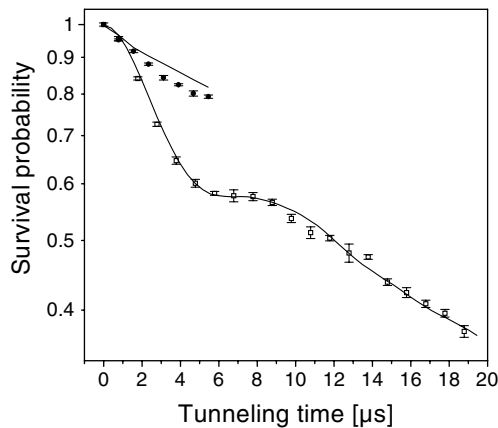


FIG. 3. Probability of survival in the accelerated potential as a function of duration of the tunneling acceleration. The hollow squares show the noninterrupted sequence, and the solid circles show the sequence with interruptions of $50 \mu\text{s}$ duration every $1 \mu\text{s}$. The error bars denote the error of the mean. The data have been normalized to unity at $t_{\text{tunnel}} = 0$ in order to compare with the simulations. The solid lines are quantum mechanical simulations of the experimental sequence with no adjustable parameters. For these data the parameters were $a_{\text{tunnel}} = 15\,000 \text{ m/s}^2$, $a_{\text{interr}} = 2000 \text{ m/s}^2$, $t_{\text{interr}} = 50 \mu\text{s}$, and $V_0/h = 91 \text{ kHz}$, where h is Planck's constant.

was limited by electronic and electro-optic devices used in the experiment. The frequency response was measured and the resulting transfer function was used to calibrate the response of the optical potential to a desired change in acceleration. This ensured that only sections were included for which tunneling was substantial and established a lower bound for the actual tunneling duration. This effect was taken into account for the curves in Fig. 3. Also indicated as solid lines are quantum mechanical simulations of the decay by numerically integrating Schrödinger's equation for the experimental sequence and determining the survival probability numerically. The simulations contained no adjustable parameters and are in good agreement with the experimental data. We attribute the seemingly larger decay rate for the Zeno experiment, as compared to the simulation, to the underestimate of the actual tunneling time. This suggests that in reality the decay might be even slower than indicated by the experimental data points.

The shape of the uninterrupted decay curve suggests yet another option for changing the decay behavior of an unstable system. After an initial period of slow decay, the curve shows a steep drop as part of an oscillatory feature, which for longer time damps away to show the well-known exponential decay. If the system was to be interrupted right after the steep drop, one would expect an overall decay that is faster than the uninterrupted decay [9]. In contrast to the slower decay for the Zeno effect this prediction was named the anti-Zeno effect. The solid circles in Fig. 4 show such a decay sequence, where after every $5 \mu\text{s}$ of tunneling the decay was interrupted by a slow acceleration segment. As in the Zeno case, these interruption segments force the system to repeat the initial nonexponential de-

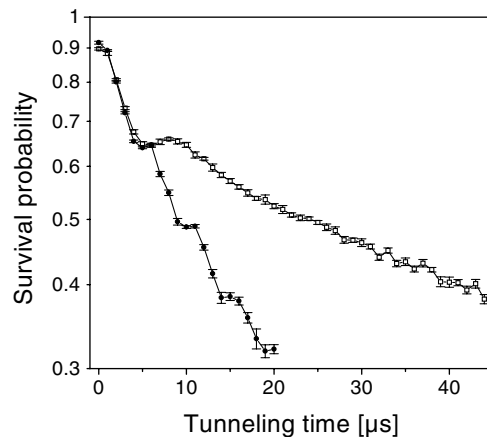


FIG. 4. Survival probability as a function of duration of the tunneling acceleration. The hollow squares show the noninterrupted sequence, and the solid circles show the sequence with interruptions of $40 \mu\text{s}$ duration every $5 \mu\text{s}$. The error bars denote the error of the mean. The experimental data points have been connected by solid lines for clarity. For these data the parameters were: $a_{\text{tunnel}} = 15\,000 \text{ m/s}^2$, $a_{\text{interr}} = 2800 \text{ m/s}^2$, $t_{\text{interr}} = 40 \mu\text{s}$, and $V_0/h = 116 \text{ kHz}$.

cay behavior after every measurement. Here, however, the tunneling segments between the measurements are chosen longer in order to include the periods exhibiting fast decay. The overall decay is much faster than for the uninterrupted case, indicated by the hollow squares in the same figure.

The key to observing the Zeno and anti-Zeno effects is the ability to measure the state of the system in order to repeatedly redefine a new initial state. In our case the measurement is done by separating in momentum space the atoms still left in the unstable state from the ones that decayed into the reservoir. In order to distinguish the two classes of atoms, they must have a separation of at least the size of the momentum distribution of the unstable state, which in our case is the width of the first Brillouin zone of $\delta p = 2m v_{\text{rec}}$. The time it takes for an atom to be accelerated in velocity by this amount is the Bloch period $\tau_b = 2v_{\text{rec}}/a_{\text{interr}}$, assuming an acceleration of a_{interr} . An interruption shorter than this time will not resolve the tunneled atoms from those still trapped in the potential and therefore results in an incomplete measurement of the atom number. To investigate the effect of the interruption duration we repeated a sequence to measure the anti-Zeno effect for varying interruption durations while holding all other parameters constant. Figure 5 displays the results of this measurement, interrupting the decay every $5 \mu\text{s}$ with an acceleration of a_{interr} of 2000 m/s^2 . The hollow squares show the uninterrupted decay sequence as a reference. For an interruption duration smaller than the Bloch period of $30 \mu\text{s}$ the measurement of the atom number is incomplete and has little or no effect. For a duration longer than the Bloch period the effect saturates and results in a complete restart of the decay behavior after every interruption. Even though this method of interruption is not an instantaneous measurement of the state of the unstable system, we can

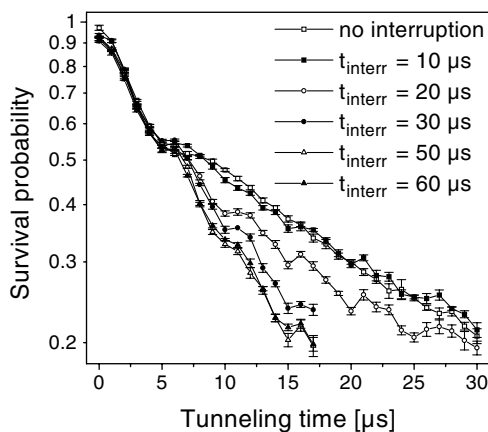


FIG. 5. Survival probability as a function of duration of the tunneling acceleration. The hollow squares show the noninterrupted sequence, and the other symbols indicate the sequence with a finite interruption duration after every $5 \mu\text{s}$ of tunneling. The error bars denote the error of the mean. A further than indicated increase of the interruption duration does not result in a further change of the decay behavior. The experimental data points have been connected by solid lines for clarity. For these data the parameters were $a_{\text{tunnel}} = 15\,000 \text{ m/s}^2$, $a_{\text{interr}} = 2000 \text{ m/s}^2$, and $V_0/h = 91 \text{ kHz}$.

still accomplish the task of redefining the initial state by first switching the system from an unstable to a stable one, then in a finite time perform the measurement and finally switching the system back again to unstable.

One of us (M. G. R.) thanks Gershon Kurizki and Abraham Kofman for helpful discussions. This work was supported by NSF, the R. A. Welch Foundation, and the Sid W. Richardson Foundation.

- [1] R. G. Winter, Phys. Rev. **123**, 1503 (1961).
- [2] L. Fonda, G. C. Ghirardi, and A. Rimini, Rep. Prog. Phys. **41**, 587 (1978).
- [3] Q. Niu and M. G. Raizen, Phys. Rev. Lett. **80**, 3491 (1998).
- [4] B. Misra and E. C. G. Sudarshan, J. Math. Phys. **18**, 756 (1977).
- [5] C. B. Chiu, E. C. G. Sudarshan, and B. Misra, Phys. Rev. D **16**, 520 (1977).
- [6] J. J. Sakurai, *Modern Quantum Mechanics* (Addison-Wesley, Reading, MA, 1994).
- [7] W. C. Schieve, L. P. Horwitz, and J. Levitan, Phys. Lett. A **136**, 264 (1989).
- [8] A. G. Kofman and G. Kurizki, Phys. Rev. A **54**, R3750 (1996).
- [9] A. G. Kofman and G. Kurizki, Nature (London) **405**, 546 (2000).
- [10] P. Facchi, H. Nakazato, and S. Pascazio, Phys. Rev. Lett. **86**, 2699 (2001).
- [11] Q. Niu, X. Zhao, G. A. Georgakis, and M. G. Raizen, Phys. Rev. Lett. **76**, 4504 (1996).
- [12] S. R. Wilkinson, C. F. Bharucha, K. W. Madison, Q. Niu, and M. G. Raizen, Phys. Rev. Lett. **76**, 4512 (1996).
- [13] C. F. Bharucha, K. W. Madison, P. R. Morrow, S. R. Wilkinson, B. Sundaram, and M. G. Raizen, Phys. Rev. A **55**, R857 (1997).
- [14] S. R. Wilkinson, C. F. Bharucha, M. C. Fischer, K. W. Madison, P. R. Morrow, Q. Niu, B. Sundaram, and M. G. Raizen, Nature (London) **387**, 575 (1997).
- [15] W. M. Itano, D. J. Heinzen, J. J. Bollinger, and D. J. Wineland, Phys. Rev. A **41**, 2295 (1990).
- [16] P. Kwiat, H. Weinfurter, T. Herzog, A. Zeilinger, and M. A. Kasevich, Phys. Rev. Lett. **74**, 4763 (1995).
- [17] C. Cohen-Tannoudji, in *Fundamental Systems in Quantum Optics*, edited by J. Dalibard, J. Raimond, and J. Zinn-Justin (Elsevier, New York, 1992).